

Delayed lanthanide luminescent Tb(III) complexes formed from lower rim amide functionalised calix[4]arenes

Christophe Lincheneau^{a†}, Eoin Quinlan^a, Jonathan A. Kitchen^{a††}, Thomas McCabe^a, Susan E. Matthews^{b*} and Thorfinnur Gunnlaugsson^{a*}

^aSchool of Chemistry, Trinity Biomedical Science Institute, Trinity College Dublin, Dublin 2, Ireland; ^bSchool of Pharmacy, University of East Anglia, Norwich, UK

(Received 29 April 2013; final version received 15 May 2013)

The synthesis and the photophysical studies of a new generation of time resolved luminescent systems based on calix[4]arenes alkylated at the lower rim, capable of hosting lanthanide (III) ions such as terbium and sensitising its emission, are described. Two series of ligands were designed to provide an ideal cavity to host terbium (Tb(III)) and were synthesised in high yields following two novel approaches. The tetra-alkylation, which was achieved in one step using with piperidino- and morpholino-acetamide pendant arms, provides eight donor atoms forming a binding ‘pocket’ at an ideal distance from the metal core to favour the sensitisation via the antenna effect. Of the two ligand series developed, compounds **3** and **4** possess a short spacer between the calix and the amide receptor site. The second series of ligands **6–7**, designed with longer pendant amide arms, was synthesised from **2** in two steps through the ester analogue **5**. The crystal structure of **3** (and **6** as shown in Supporting Information, available online) is presented. The synthesis and the photophysical studies of the four resulting complexes **3.Tb**, **4.Tb**, **6.Tb** and **7.Tb** are described in detail and in each case, successful sensitisation of the terbium emission occurred upon excitation of the phenolic scaffold of the calixarene.

Keywords: supramolecular chemistry; calix[4]arenes; lanthanide; terbium complexes; solution studies; luminescence

Introduction

Over the past few decades, the use of lanthanide ions has become an important strategy for the development of sensors and probes for use in *in vivo* applications, such as in time-delayed luminescent chemosensing and imaging, as well as in the development of targeted magnetic resonance imaging (MRI) contrast agents (**1–3**). A wide variety of ligand platforms including cyclen (**4**) and cryptands (**5**) have been investigated along with acyclic podands (**6**), and more recently, self-assembly, where lanthanides have been employed to direct the synthesis of various luminescent architectures, has been exploited (**7**).

Calixarenes are highly attractive platforms due to their ease of functionalisation and spatial pre-organisation. These platforms have proved highly effective in the development of lanthanide extractants particularly for nuclear waste remediation (**8**) and in the development of MRI contrast agents (**9**). The earliest examples of luminescent complexes, from the groups of Shinkai (**10**) and Ungaro (**11**), featured amide residues at the lower-rim

and demonstrated high-quantum yields which, in some cases, could be tailored by introduction of a sensitising unit. Subsequently, both simple carboxylates (**12**) and amines (**13**) have also been investigated. In an alternative approach, known lanthanide ligands such as heterocyclic *N*-oxides (**14**), 2,2'-bipyridines (**15**) and dipicolinates (**16**) have been incorporated to afford efficient binding and energy transfer. More recently, the exploitability of calixarene-based ligands has been increased by the use of water-soluble calixarene scaffolds (**17**) and through direct incorporation in polymers for the synthesis of hybrid materials (**18**) and through the development of near-infrared luminescent sensors (**19**). In their original work, Shinkai and coworkers (**10**) proposed that sensitisation of the lanthanide excited state could occur via two different pathways, depending on the nature of the lanthanide ion, as shown in **Figure 1**. Path A, used in the case of Tb(III), involves excitation of the phenolic scaffold followed by an intersystem crossing towards the $^3\pi-\pi^*$ of the calixarenes, with subsequent population of the 5D_4 excited states

*Corresponding authors. Email: Susan.Matthews@uea.ac.uk; gunnlaut@tcd.ie

[†]Present address: Christophe Lincheneau, Photochemical Nanosciences Laboratory, Dipartimento di Chimica “G. Ciamician”, Università di Bologna, Via Selmi 2, 40126 Bologna, Italy.

^{††}Present address: Jonathan A. Kitchen, Department of Chemistry, Faculty of Natural & Environmental Sciences, University of Southampton, Highfield, Southampton SO17 1BJ, UK.

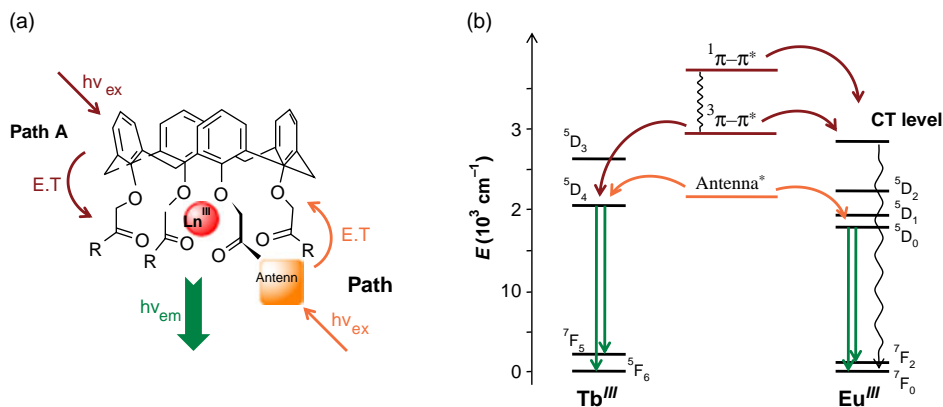


Figure 1. (a) Lanthanide emission sensitisation process. Path A in the case of Tb(III) and Path B for Eu(III). (b) Jablonski diagram for the sensitisation of lanthanide luminescence using the Path A (in red) and Path B (in orange).

of Tb(III) (*12c,14*) giving rise to quantum yields of 10–20% in water. However, in the case of Eu(III), the carbonyl C=O binding to Eu(III) was found to give rise to charge transfer levels, which were populated from either the $^1\pi\pi^*$ or the $^3\pi\pi^*$ excited states of the calix-ligand, and this gave rise to deactivation of the Eu(III) emission via a non-radiative process and hence quenching of the luminescence emission. Although these difficulties can be overcome through inclusion of another antenna possessing lower excited triplet states, an alternative approach is to provide an extended complexation cavity. In this paper, we report the synthesis of a new family of lower-rim calixarene derivatives, featuring an eight electron donor cavity with optimised geometry to host Tb(III), and the investigation of their luminescent properties.

Experimental section

General procedures

^1H NMR spectra were recorded using 400 MHz instrument or 600.1 MHz; ^{13}C NMR were recorded at 100 or 150.2 MHz. Mass spectrometry was carried out using HPLC grade solvents using an electrospray spectrometer in a positive mode. High-resolution mass spectra were determined relative to a standard of leucine enkephaline. Crystal for X-ray diffraction was analysed and solved in-house. High-grade solvents (methanol and acetonitrile) were used for the synthesis of the ligand and complex. Analytical thin-layer chromatography was performed using silica gel plates. Visualisation was by UV light (254 nm), by exposure to iodine vapour, immersion aqueous alkaline KMnO_4 solution or with a 2% ninhydrin in ethanol spray reagent. Columns were run using Silica gel 60 (230–400 mesh). All lanthanide luminescent spectra were in phosphorescent mode with a gate time of 5 ms and slit widths of 10 or 20 nm.

Synthesis

25,26,27,28-Tetrakis[(N-piperidinyl)carbonyl)methoxy]calix[4]arene (**3**)

The calix[4]arene (**2**) (500 mg, 1.18 mmol) was reacted with 2-bromoacetyl piperidine (1.1 g, 5.34 mmol) and K_2CO_3 (1.0 g, 7 mmol) in CH_3CN (30 mL). Heating at reflux temperature overnight gave a coffee-coloured suspension. Workup followed by crystallisation from CH_3OH gave the title compound as a cream solid (523 mg, 48%) (m.p.: 291°C) (dec.). ^1H NMR (400 MHz, CDCl_3 , δ_{H}): 6.64–6.60 (m, 12H, Ar–H), 5.11 (d, $J = 14.1$ Hz, 4H, Ar– CH_2 –Ar), 4.90 (s, 8H, $\text{OCH}_2\text{C}(\text{O})$), 3.52 (t, $J = 5.0$ Hz, 8H, N [CH_2CH_2] CH_2), 3.43 (t, $J = 5.0$ Hz, 8H, N [CH_2CH_2] CH_2), 3.26 (d, $J = 13.8$ Hz, 4H, Ar– CH_2 –Ar), 1.64 (m, 8H, N [CH_2CH_2] CH_2), 1.56 (bs, 16H, N [CH_2CH_2] CH_2). ^{13}C NMR (100 MHz, CDCl_3 , δ_{C}): 167.3, 155.9, 134.3, 128.0, 121.8, 71.2, 45.2, 42.1, 31.4, 25.9, 25.1, 24.2. IR (ν , cm^{-1}): 2919, 2848, 1663, 1464, 1204, 1008, 761, 752. ES-MS (m/z): 947.46 (M + Na). Required for $\text{C}_{56}\text{H}_{68}\text{N}_4\text{O}_8$: C, 72.70; H, 7.41; N, 6.06. Found: C, 72.49; H, 7.43; N, 5.99.

25,26,27,28-Tetrakis[(N-morpholino)carbonyl)methoxy]calix[4]arene (**4**)

To a suspension of calix[4]arene (**2**) (1.0 g, 2.36 mmol) in acetonitrile (50 mL) was added K_2CO_3 (1.95 g, 14 mmol) and 2-bromo-1-morpholinoethanone (2.94 g, 14.1 mmol). The suspension was stirred at reflux overnight, resulting in a brown suspension. Solvents were removed, and the residue was partitioned between water (100 mL) and CH_2Cl_2 (100 mL). The organic layer was removed and the water layer was extracted again with CH_2Cl_2 (50 mL). The combined organic layers were then further washed with water (100 mL) and dried (Na_2SO_4), and the solvent was removed under reduced pressure. The resulting solid was recrystallised from ethanol to give the title compound

(1.44 g, 66%) (m.p.: 218°C). ^1H NMR (400 MHz, CDCl_3 , δ_{H}): 6.60–6.67 (m, 12H, Ar–H), 4.98 (d, $J = 14$ Hz, 4H, Ar– CH_2 –Ar), 4.91 (s, 4H, ArO– CH_2 –C(O)), 3.49–3.69 (m, 32H, N(CH_2CH_2) $_2$ O), 3.26 (d, $J = 14$ Hz, Ar– CH_2 –Ar). ^{13}C NMR (100 MHz, CDCl_3 , δ_{C}): 167.6, 155.4, 134.1, 128.1, 122.2, 70.8, 66.4, 66.2, 44.4, 41.2, 31.1. IR (ν , cm^{-1}): 3445, 2967, 2912, 2863, 1676, 1658, 1466, 1448, 1466, 1358, 1299, 1274, 1213, 1236, 1196, 1112, 1095, 1068, 1026, 998, 911, 852, 778, 754. ES-MS (m/z): 955.38 (M + Na). Required for $\text{C}_{52}\text{H}_{60}\text{N}_4\text{O}_{12}\cdot\text{H}_2\text{O}$: C, 65.67; H, 6.57; N, 5.89. Found: C, 65.88; H, 6.49; N, 5.65.

25,26,27,28-Tetrakis-N-(piperidinyl-2-aminoethyl) carbamoyloxymethoxycalix[4]arene (**6**)

Yield: 556 mg (78%), white powder (m.p.: 201°C). ^1H NMR (400 MHz, CDCl_3 , δ_{H}): 7.63 (bs, 4H, NH), 6.61 (m, 12H, Ar–H), 4.49 (d, $J = 13.8$ Hz, 4H, Ar– CH_2 –Ar), 4.46 (s, 8H, ArO– CH_2 –CO), 3.47 (q, $J = 6.5$ Hz, 8H, –NH– CH_2 – CH_2), 3.26 (d, $J = 13.8$ Hz, 4H, Ar– CH_2 –Ar), 2.50 (t, $J = 6.5$ Hz, 8H, NH– CH_2 – CH_2), 2.39 (bs, 16H, N(CH_2CH_2) CH_2), 1.52 (m, 16H, N(CH_2CH_2) $_2\text{CH}_2$), 1.43 (m, 8H, N(CH_2CH_2) $_2\text{CH}_2$). ^{13}C NMR (100 MHz, CDCl_3 , δ_{C}): 169.0, 133.8, 128.4, 122.7, 73.7, 57.2, 54.0, 35.9, 30.6, 25.5, 23.9. IR (ν , cm^{-1}): 3284, 2930, 2949, 2773, 1657, 1550, 1440, 1350, 1319, 1304, 1245, 1198, 1159, 1130, 1087, 1053, 1036, 1011, 831, 770, 758. Accurate MS (m/z) – calculated: 1098.6876 (M/2) + H; found: 1098.6882. Analysis (%) – required for $\text{C}_{64}\text{H}_{88}\text{N}_8\text{O}_8$ 1/2Et $_2$ O: C, 69.87; H, 8.26; N, 9.88. Found: C, 69.90; H, 8.08; N, 10.24.

25,26,27,28-Tetrakis-N-((4-piperazinyl)-2-aminoethyl) carbamoyloxymethoxy calix[4]arene (**7**)

Yield: 314 mg (44%), hygroscopic white powder; m.p.: 98°C. ^1H NMR (400 MHz, CDCl_3 , δ_{H}): 7.64 (s, 4H, NH), 6.63 (m, 12H, Ar–H), 4.51 (d, 4H, Ar– CH_2 –Ar), 4.48 (s, 8H, ArO– CH_2 –C(–O)N), 3.48 (q, $J = 6$ Hz, H [N CH_2CH_2]N), 3.46 (d, $J = 14$ Hz, 4H, Ar– CH_2 –Ar), 2.90 (m, 16H, N[CH_2CH_2]N), 2.54 (t, $J = 6$ Hz, HN [CH $_2\text{CH}_2$]N), 2.42 (m, 16H N[CH $_2\text{CH}_2$]N). ^{13}C NMR (100 MHz, CDCl_3) δ_{C} : 169.1, 133.7, 128.4, 122.8, 73.6, 57.1, 53.9, 45.6, 45.4, 35.6, 30.6. IR (ν , cm^{-1}): 3301, 3062, 2912, 2850, 2809, 1659, 1538, 1439, 1244, 1194, 1115, 1094, 1009, 867, 852, 778, 761. Accurate MS (m/z) – calculated: 1102.6730 (M/2) + H; found: 1102.6692.

Complex **3.Tb**

Complex **3.Tb** was synthesised by refluxing ligand **3** (14.1 mg, 1.5×10^{-5} mol) with Tb(ClO_4) $_3$ (11.8 mg, 1.5×10^{-5} mol) in methanol (10 mL) to yield **3.Tb** as a white solid (14.2 mg, 69%) after precipitation from methanol

upon the addition of diethylether. Melting point decomposed above 280°C. Calculated for $\text{C}_{56}\text{H}_{68}\text{Cl}_3\text{N}_4\text{O}_{20}\text{Tb}$: C, 48.65; H, 4.96; N, 4.05. Found: C, 48.43; H, 4.85; N, 3.95. HR-MS calculated for $\text{C}_{56}\text{H}_{68}\text{Cl}_2\text{N}_4\text{O}_{16}\text{Tb} [\text{M}^{3+} + 2\text{ClO}_4^-]^+$ (m/z) = 1281.3261. Found: 1281.8023; δ_{H} (CD_3CN ; 400 MHz): 7.28, 6.61, 5.11, 4.89, 3.51, 3.42, 3.27; IR ν_{max} : 2945, 2857, 1645, 1616, 1500, 1440, 1370, 1278, 1177, 1082, 1001, 952, 901, 856, 783.

Complex **4.Tb**

Complex **4.Tb** was synthesised by refluxing **4** (8.9 mg, 0.9×10^{-5} mol) with Tb(ClO_4) $_3$ (7.38 mg, 1.5×10^{-5} mol) in methanol (10 ml) yielding **4.Tb** as a white solid (11.4 mg, 99%) after precipitation from methanol using diethylether. Melting point decomposed above 280°C. Calculated for $\text{C}_{52}\text{H}_{60}\text{Cl}_3\text{N}_4\text{O}_{24}\text{Tb}$: C, 44.92; H, 4.35; N, 4.03. Found: C, 44.85; H, 4.28; N, 4.01. HR-MS calculated for $\text{C}_{52}\text{H}_{60}\text{Cl}_2\text{N}_4\text{O}_{20}\text{Tb} (\text{M}^{3+} + 2\text{ClO}_4^-)$ (m/z) 1289.2431. Found: 1289.8 [M $^{3+} + 2\text{ClO}_4^-$] $^+$; δ_{H} (CD_3CN ; 400 MHz): 7.28, 6.80, 6.67, 4.81, 3.61, 3.37, 3.26; IR ν_{max} : 2965, 2930, 2853, 1680, 1673, 1486, 1370, 1320, 1280, 1220, 1200, 1000, 920, 780, 750.

Complex **5.Tb**

Complex **5.Tb** was synthesised by refluxing ligand **5** (20.9 mg, 1.8×10^{-5} mol) with Tb(ClO_4) $_3$ (14.9 mg, 1.8×10^{-5} mol) in methanol (10 mL) yielding **5.Tb** as a hygroscopic white solid (27.4 mg, 97%) after precipitation from methanol upon the addition of diethylether. Melting point decomposed above 280°C. Calculated for $\text{C}_{64}\text{H}_{88}\text{Cl}_3\text{N}_8\text{O}_{20}\text{Tb}$: C, 49.44; H, 5.71; N, 7.21. Found: C, 48.38; H, 5.74; N, 7.18. HR-MS calculated for $\text{C}_{64}\text{H}_{88}\text{Cl}_3\text{KN}_8\text{O}_8\text{Tb} [\text{M}^{3+} + 3\text{Cl}^- + \text{K}^+]$ (m/z) = 1399.4531. Found: 1399.3651 δ_{H} (CD_3CN ; 400 MHz): 7.29, 6.62, 4.53, 3.55, 2.52, 2.12; IR ν_{max} : 3290, 2940, 2860, 1660, 1634, 1579, 1459, 1443, 1390, 1280, 1250, 1177, 1056, 943, 903, 856, 821, 777, 716, 691.

Complex **6.Tb**

Complex **6.Tb** was synthesised by refluxing ligand **6** (28.2 mg, 2.6×10^{-5} mol) with Tb(ClO_4) $_3$ (20.1 mg, 2.6×10^{-5} mol) in methanol (10 mL) yielding **6.Tb** as a hygroscopic white solid (37.9 mg, 95%) after precipitation from methanol upon the addition of diethylether. Melting point decomposed above 280°C. Calculated for $\text{C}_{60}\text{H}_{84}\text{Cl}_3\text{N}_{12}\text{O}_{20}\text{Tb}$: C, 46.23; H, 5.43; N, 10.78. Found: C, 46.18; H, 5.40; N, 10.81. HR-MS: calculated for $\text{C}_{60}\text{H}_{84}\text{Cl}_3\text{KN}_{12}\text{O}_8\text{Tb} [\text{M}^{3+} + 3\text{Cl}^- + \text{K}^+]$ (m/z) = 1403.4297. Found 1403.2623; δ_{H} (CDCl_3 ; 400 MHz): 7.31, 6.56, 4.45, 3.40; 3.22; 2.85 2.46; IR ν_{max} : 3320, 3080, 2945, 2880, 2830, 1681, 1560, 1450, 1205, 880, 795, 760.

Crystallographic analysis

X-ray data for ligand **3** (CCDC no. 916512) were collected on a Bruker SMART APEX CCD diffractometer using graphite-monochromated Mo K α radiation ($\lambda = 0.71073 \text{ \AA}$). The data sets were processed and corrected for Lorentz and polarisation effects using SMART and SAINT-PLUS software. The structures were solved using direct methods with the SHELXTL program package and refined against all F^2 data. All H-atoms were positioned geometrically and refined using a riding model with $d(\text{CH}_{\text{aro}}) = 0.95 \text{ \AA}$, $U_{\text{iso}} = 1.2U_{\text{eq}}$ (C) for aromatic, and 0.99 \AA , $U_{\text{iso}} = 1.2U_{\text{eq}}$ (C) for CH_2 .

Results and discussion

Synthesis and characterisation of the ligands 3–7

With the aim of developing a new generation of luminescent probes for time-resolved imaging, the two families of calix[4]arenes **3**, **4** and **5–7** shown in Figure 2 were designed to provide an octadentate binding pocket capable of hosting terbium below the rim of the calixarene moiety. Here, the tetra-alkylation of the lower rim of the calixarene provides eight donor atoms for both types of receptors; the first receptor via the four phenolic oxygens and the four amido moieties, chosen as amido-piperidine (**3**) and amido-morpholine (**4**), and for the second systems,

a longer chain was employed giving the ethylene-piperidine (**6**) and ethylene-piperazyl (**7**) structures. The calixarene **2** (**20**) was synthesised from the commercially available cyclic tetramer **1** in a conventional way. Ligands **3** and **4** were designed with shorter arms containing amido-piperidine and amido-morpholine terminal moieties close from the lanthanide binding pockets. Employing Williamson ether-synthesis, using the appropriate α -bromoacetamides [For examples of the use of such synthesis, see Ref. (21).] gave **3** and **4** in 48% and 66% yields, respectively, after trituration using diethylether. In both cases, the successful tetra functionalisation and the resulting C_{4v} symmetry was observed from the ^1H NMR analysis as shown in Figure 3(a),(b). The resonances of the aromatic protons coalesce into a broad multiplet at 6.60–6.50 ppm in both cases. The protons in the α -position of the amido moiety, which are subjected to strong shielding due to the presence of the phenolic ether and the amido moiety, were observed as a singlet at 4.90 and 4.92 ppm for **3** and **4**, respectively. The CH_2 methylene bridges of the calixarene resonated as two doublets ($^2J = 14 \text{ Hz}$) at 5.11 and 3.26 ppm ($\delta_{\text{H}} = 4.98$, $\delta_{\text{H}} = 3.26 \text{ ppm}$ and $^2J = 14 \text{ Hz}$ for **4**) which are indicative of *exo*- and *endo*-environments for each of these protons. This confirmed the cone conformation of calix[4]arenes **3** and **4**.

The purity of both ligands was also confirmed using traditional characterisation methods; furthermore,

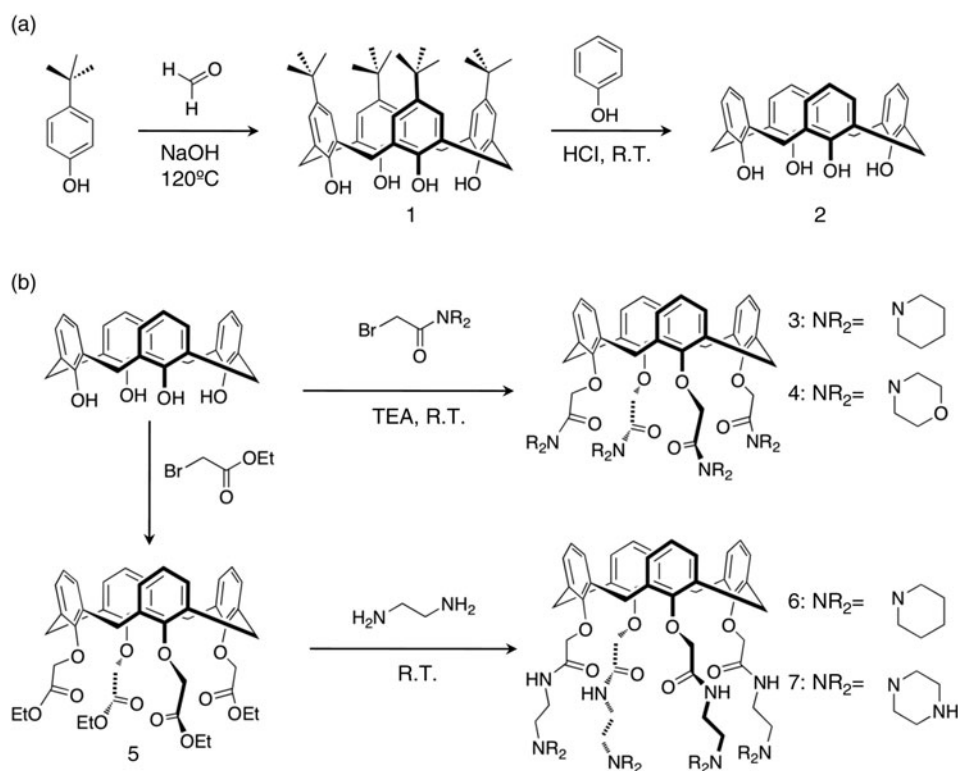


Figure 2. (a) Synthesis of the calix[4]arene **2** in two steps. (b) Synthesis of the calix[4]arene derivatives **3–7** from the calixarene **2**.

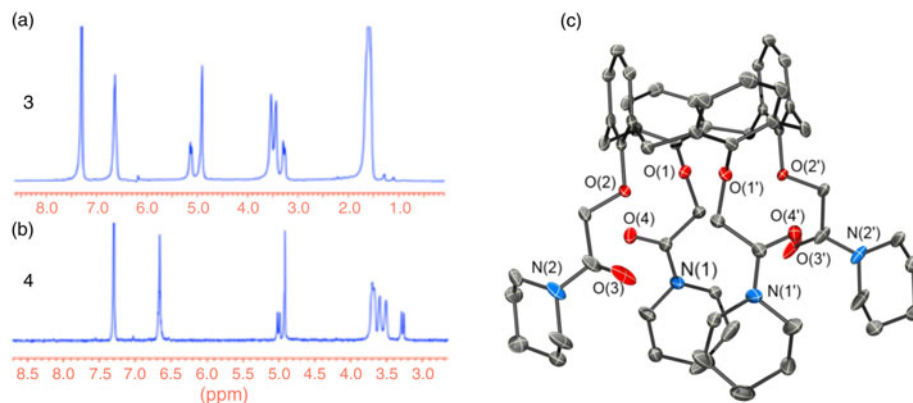


Figure 3. (Colour online) The ^1H NMR (CDCl_3 ; 400 MHz) spectra of ligands **3** (a) and **4** (b). (c) Perspective view of **3** with thermal ellipsoids set at 30% probability. Hydrogen atoms and minor components of disorder are omitted for clarity.

colourless plate-shaped crystals of **3** suitable for single X-ray crystal structure analysis were obtained via slow evaporation at room temperature from a mixture of $\text{CH}_2\text{Cl}_2/\text{MeOH}$ solution. Compound **3** crystallised in the monoclinic space group $C2/c$ and contained half of one molecule in the asymmetric unit with the other half generated by a twofold rotation axis (Figure 3(c)). The crystal structure of **3** contains disorder at the piperidine ring of N(1) where two of the carbon atoms are each disordered over two sites, C(6)/C(9) and C(66)/C(99) with relative occupancies of 0.65 and 0.35, respectively (see Supporting Information, available online for figure). In addition, the carbonyl oxygen atom on the other piperidine-containing arm is also disordered over two sites where O(3) and O(33) have relative occupancies of 0.5 and 0.5, respectively (see Supporting Information, available online for figure). The calix component of **3** adopts a pronounced 'boat' configuration where two of opposite aromatic rings are 'flattened' with inter-centroid distances determined as 5.15 Å apart between the 'pinched' rings, whereas the 'flattened' ring centroids are 7.67 Å apart. The packing observed when viewed along the crystallographic c -axis (see Supporting Information, available online) showed the formation of a ribbon-like packing array, whereby the calix[4]arene aromatic core and the aliphatic piperidine moieties alternate in a head-to-tail fashion. The solid-state structure showed a cavity of *ca.* 6.4 Å (measured diagonally between the coordinating amido oxygens), which should allow for the inclusion of a cationic guest such as terbium. However, the piperidine moieties, which are in close proximity to the binding site, may impart strain on the system lowering the affinity towards the lanthanide guest.

The second series of ligands **6–7** was designed with an ethylene spacer between the binding pocket and the terminal moiety in order to add more flexibility to the pendant arms and minimise the strain due to the presence of the terminal moieties. The calixarenes **6** and **7** were

synthesised as shown in Figure 2(b) from the known tetra ester **5** (22). The nucleophilic substitution of the ester moiety, using the pure amine, allowed the formation of the calix[4]arenes **6–7** in respectively 44% and 78% yields. The ^1H NMR analysis of each ligand gave similar results as for the shorter analogues **3** and **4**. As shown in Figure 4 (a),(b), the simplicity of the NMR reflects the C_4 symmetry of these structures with the phenolic protons coalescing within the 6.60–6.50 ppm range, whereas the CH_2 of the calixarene scaffold occurred as a set of doublets at 5.11 and 3.26 ppm for **6**, and at 4.53 and 3.26 ppm for **7**. In the case of compound **6**, small poor-quality crystals were obtained by slow vapour diffusion of di-isopropylether into CH_2Cl_2 ; however, the data obtained from diffraction studies were limited and only the connectivity could be

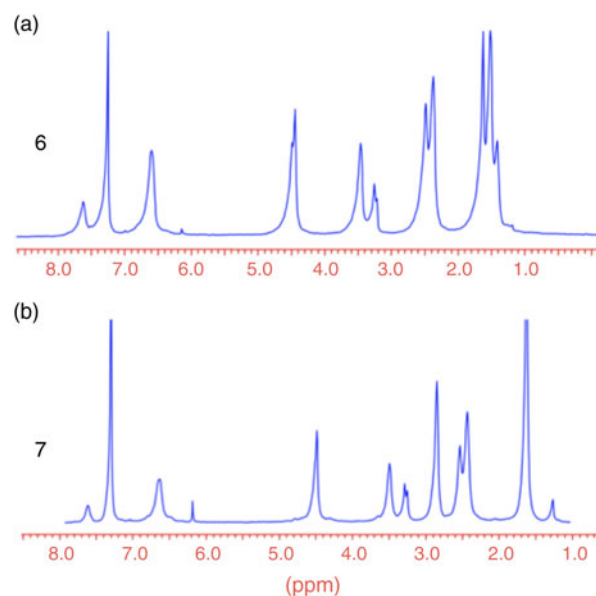


Figure 4. (Colour online) The ^1H NMR (CDCl_3 ; 400 MHz) spectra of ligands **6** (a) and **7** (b).

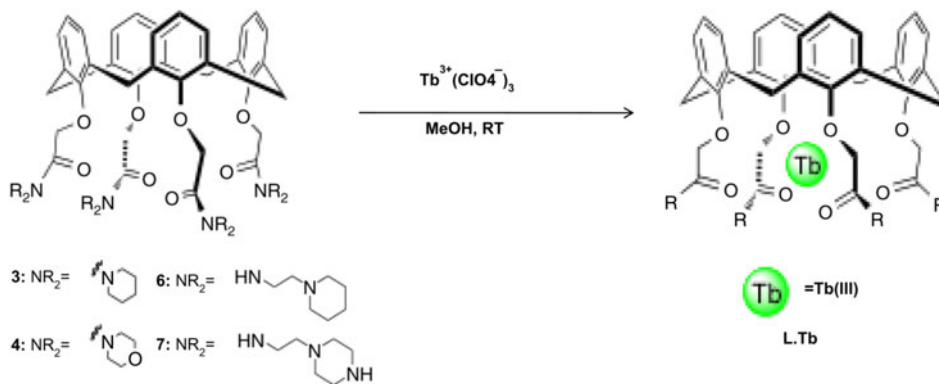


Figure 5. (Colour online) The synthesis of the complexes **3.Tb**, **4.Tb**, **6.Tb** and **7.Tb** from ligands **3**, **4**, **6** and **7**, respectively.

determined from the data. Although no detailed structural information is discussed, it is clear that the calixarene portion of **6** also adopted a boat-like configuration in the solid state (the structure is shown in Supporting Information, available online).

Synthesis and characterisation of *L.Tb* (*L* = **3**, **4**, **6**, **7**)

The synthesis of the complexes *L.Tb* was carried out in MeOH as described in Figure 5. The complexes were isolated via precipitation from diethylether in high yield of 90–95%, except in the case of **4.Tb**, which precipitated in solution after 5 min stirring in 67% yield. The characterisation of the complexes *L.Tb* (*L* = **3**, **4**, **6** and **7**) was achieved using conventional spectroscopic methods. Using MS analyses (ESI + /ToF mode in MeOH), the complexes **3.Tb** and **4.Tb** were detected as a mono- and di-charged fragments, corresponding to $M^{3+} + 2ClO_4^-$ and $M^{3+} + ClO_4^-$ ions, respectively, whereas the **6.Tb** and **7.Tb**, containing the longer arms, were found as a mono-charged ions, corresponding to $M^{3+} + 3Cl^- + K^+$.

Furthermore, for each of these complexes, the observed ES-MS showed the characteristic isotopic distribution pattern of monometallic Tb(III) complexes which matched that of the calculated isotopic distribution pattern, indicating the successful formation of the complex in 1:1 stoichiometry, as shown in Figure 6 for **3.Tb**–**7.Tb**.

The conformation of *L.Tb* was further investigated using 1H NMR spectroscopy ($CDCl_3$, 400 MHz). In all cases (Figure 7), the 1H NMR spectrum was broad, but not greatly shifted, and each showed a species of high symmetry, reflecting the C_4 symmetrical nature of these structures, and hence, the retention of the *cone* conformation observed in the 1H NMR of the ligands. Having established the successful formation of these Tb(III) complexes, we next evaluated their photophysical properties in solution.

Photophysical studies of the complexes *L.Tb* (*L* = **3**, **4**, **6**, **7**)

The photophysical properties of the ligands and the Tb(III) *L.Tb* (*L* = **3**, **6** and **7**) complexes were investigated in

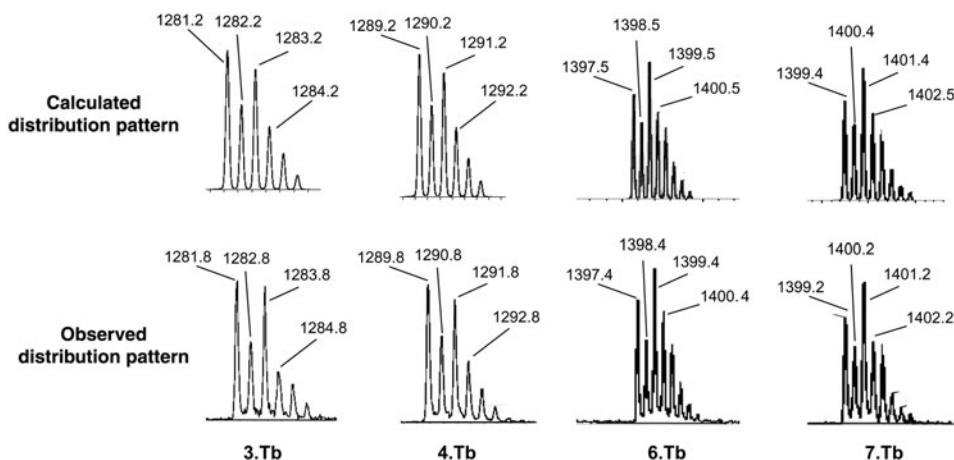


Figure 6. Calculated and observed isotopic distribution pattern of the complexes *L.Tb* (*L* = **3**, **4**, **6** and **7**), demonstrating the formation of the desired 1:1 complexes.

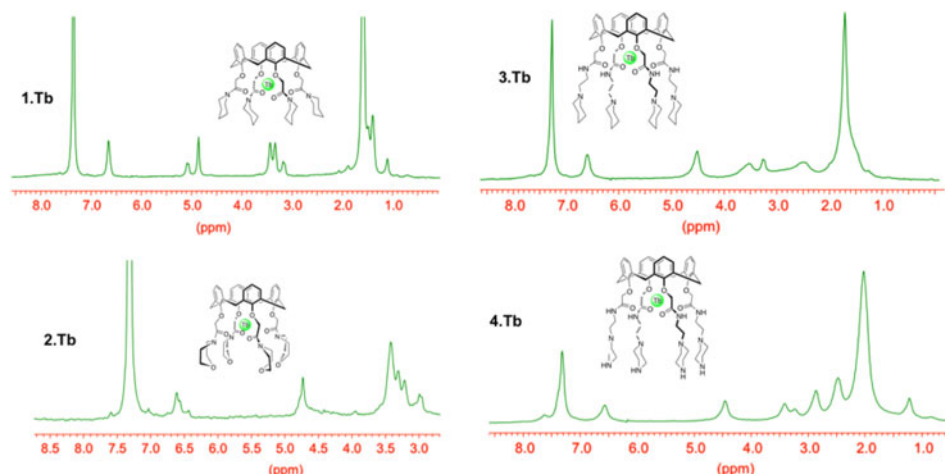


Figure 7. (Colour online) The proton NMR of the Tb(III) complexes developed in this study.

MeOH solution, whereas for **4** and **4.Tb**, the analysis was performed in a 4:1 dimethyl sulfoxide (DMSO):H₂O mixture, due to precipitation of the latter structure from MeOH. For the ligands, the UV–vis absorption spectrum showed a broad absorption band centred at λ_{max} ca. 270 nm, which was the characteristic of the $\pi \rightarrow \pi^*$ transitions of the aromatic scaffold of the calixarenes. The molar extinction coefficients ϵ_{271} were determined for each of the ligands, being $\epsilon = 2039$, 2006, 1458 and $1388 \text{ M}^{-1} \text{ cm}^{-1}$ for **3**, **4**, **6** and **7**, respectively, in the above solvent systems. These results show that **6** and **7** possessed a similar, and at the same time, a significantly smaller extinction coefficient than that determined for **3** and **4**. The excitation of the calixarene scaffold of **3**, **4**, **6** and **7** gave rise, on all occasions, to a weak and broad fluorescence emission that were centred at ca. 416 nm.

The UV–vis absorption spectra of **3.Tb** was significantly different to that seen for **3**, being ca. 70%

hypochromically effected upon complexation to Tb(III). In comparison, the UV–vis absorption spectra of **4.Tb**, **6.Tb** and **7.Tb** were structurally similar to that seen above for their respective ligands. The excitation of the calix[4]arene scaffold at 271 nm, for each of the complexes **L.Tb**, gave rise to typical Tb(III) emission demonstrating the successful population of the Tb(III) $^5\text{D}_4$ excited state, with emission bands occurring at 487, 543, 581 and 614 nm due to the deactivation of $^5\text{D}_4$ to $^7\text{F}_J$ ($J = 6-3$) (Figure 8). On all occasions, the recorded fluorescence excitation spectra matched the UV–vis absorption spectra of the corresponding ligands, confirming the successful sensitisation of the Tb(III) $^5\text{D}_4$ excited state by these ligands. In each case, the Tb(III) emission was found to be long-lived; the lifetimes recorded for the complexes **3.Tb** and **4.Tb** excited states in MeOD were longer ($\tau = 2.3-2.6$ ms) than that recorded for **6.Tb** and **7.Tb** ($\tau = 1.5-1.7$ ms). It can be concluded from these results that the

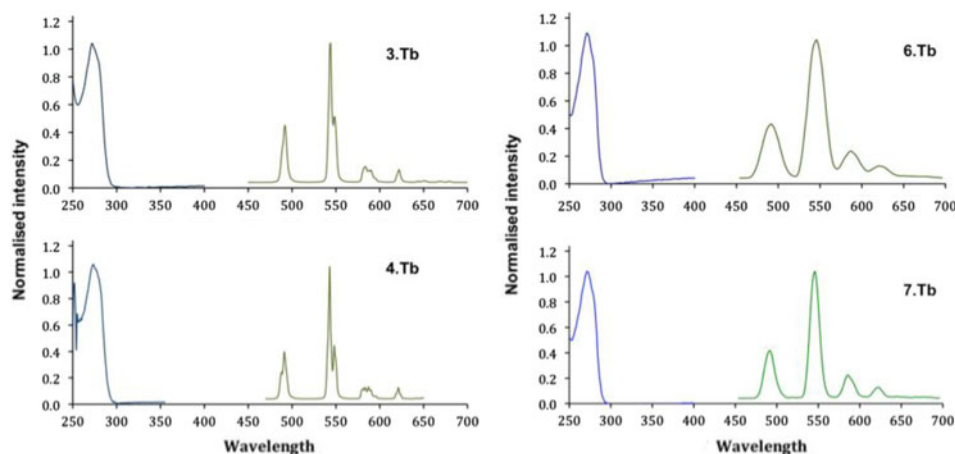


Figure 8. (Colour online) The absorption and the lanthanide luminescence emission spectra of **3.Tb**, **6.Tb** and **7.Tb** when recorded in MeOH and the same for **4.Tb** when recorded in DMSO:H₂O mixture.

Table 1. Summary of the photophysical properties of the complexes **L.Tb** (**L** = **3**, **4**, **6**, **7**) in MeOH.

Complex	3.Tb	4.Tb	6.Tb	7.Tb
ϵ_{271}	627.2	1891.9	1289.2	1206.1
ϕ (%)	19.0	18.6	0.5	0.2
τ_{MeOD}	2.325	2.593	1.759	1.457
τ_{MeOH}	1.566	2.500	1.322	1.337

non-radiative deactivation of the structure's excited states is more efficient for the complexes **6.Tb** and **7.Tb**, due to their longer pendant arms. This behaviour has been also illustrated by the luminescence quantum yield measurements, which in the case of **3.Tb** and **4.Tb** resulted in a highly luminescent terbium-centred emission with quantum yields of 19% and 18.6%, respectively, whereas in the case of **6.Tb** and **7.Tb**, the complexes were significantly less luminescent with less than 1% quantum yield as shown in Table 1.

As a consequence, the systems formed have shown the unique properties of lanthanide complexes such as an intense long-lived and narrow-shaped emission in the visible region. It was also shown that the terbium ion is hosted within the cavity formed by the four pendant arms providing eight of the nine coordination required by Tb(III). Moreover, these results suggest that the architectures **L.Tb** are good candidates for the development of sensors or time-resolved contrast agents. Having analysed the photophysical properties of these complexes, we next investigated their formation *in situ*.

Studies of the formation of the complexes **L.Tb** *in situ*

The formation of the complexes **L.Tb** was investigated *in situ* following spectroscopic methods by UV-vis absorption and lanthanide emission. The titrations were carried out by adding Tb(III) (delivered as its non-coordinating, perchlorate salt) to a solution of ligand in methanol, in the case of **3**, **6** and **7** or in a solvent mixture of

80:20 DMSO/H₂O for **6**. This involved measuring the phosphorescence intensity of the metal centre following excitation of the phenyl platform of the calixarene at 271 nm.

The changes in the absorption spectra of **3** are shown in Supporting Information (available online), where the absorption band centred at $\lambda = 271$ nm experienced a hypochromic effect, which reached a plateau after the addition of 0.7 equivalents of terbium. This can be indicative of the formation of the **3₂.Tb** at a low concentration of Tb(III). This effect was also seen in the results obtained in the luminescence titrations as shown in Figure 9(a), where the terbium luminescence of the forming complex became apparent up to the addition of 0.7 equivalents of terbium perchlorate. This confirmed the initial formation of a 1:2 (M/L) stoichiometric species followed by a displacement of the equilibrium in solution towards the 1:1 species.

The changes obtained in the spectroscopic properties of **4** upon the variation of terbium concentration (see the UV-vis changes in Supporting Information, available online) are shown in Figure 9(b), and were shown to be different to that seen above for **3**. Firstly, in the 4:1 DMSO/H₂O solvent system, no major changes were seen in the UV-vis absorption spectra of **4** upon terbium complexation (see Supporting Information, available online). However, as in the case of ligand **3**, the lanthanide luminescence is successfully switched on within the addition of 0 → 25 equivalents of terbium. Initially, the luminescence intensity increases efficiently upon the addition of 1 equivalent of Tb(III), which can be explained by the formation of the 1:1 **L/Tb** stoichiometry species, also observed in the case of the titrations of ligand **3**. The changes were then less pronounced upon the addition of Tb(III) ranging from 1 → 2 equivalents where the luminescence evolution adopted a linear increase proportional to the quantity of Tb(III) added. This is most likely due to the residual luminescence of Tb(III) perchlorate in DMSO solution after the formation of the desired 1:1 complex; but this can also be indicative of the formation of the **4.Tb₂** at higher lanthanide concentration. The complexation studies of terbium by ligands **6** and **7**

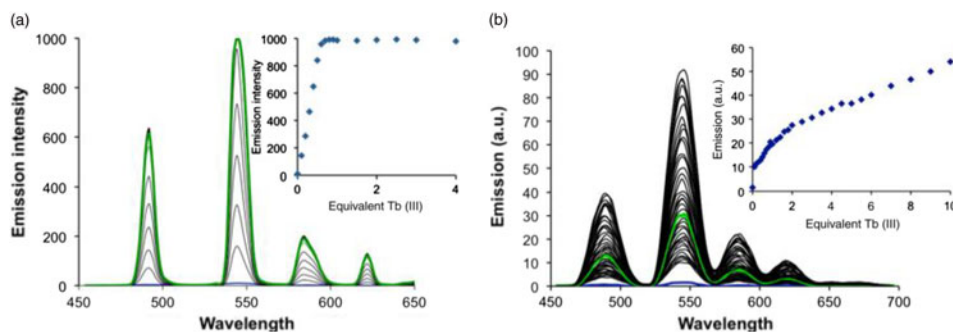


Figure 9. (Colour online) (a) Changes observed in the luminescence emission of **3** upon the addition of Tb(ClO₄)₃ in methanol. (b) Changes observed during the titration of **4** in 4:1 H₂O:DMSO mixture.

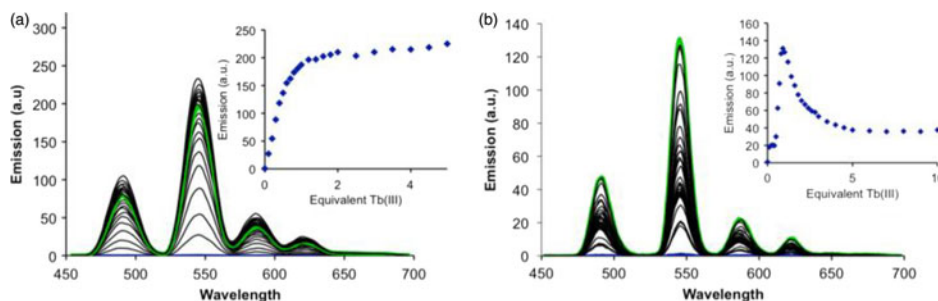


Figure 10. (Colour online) (a) Changes observed in the luminescence emission of **6** upon the addition of $\text{Tb}(\text{ClO}_4)_3$ in methanol. (b) Changes observed during the titration of **7**.

have also been investigated in MeOH. In each case, the UV–vis absorption spectrum of the ligand remained unchanged (see Supporting Information, available online). As previously shown, the terbium luminescence was switched on in the presence of lanthanide ion, indicative of $\text{Tb}(\text{III})$ complexation, signifying the formation of the complex in solution. In the case of compound **6**, the emission intensity increases upon the addition of terbium salt and reaches a plateau in the presence of one equivalent of metal suggesting the main formation of the 1:1 species **6.Tb** in solution (Figure 10(a)). However, at high concentrations of $\text{Tb}(\text{III})$, the emission intensity was weakly enhanced in proportion to the quantity of metal added, which is due to the luminescence of terbium directly excited on its UV–vis absorption band at 271 nm.

In the case of **7**, the behaviour of the luminescence emission followed a different pattern as is evident in Figure 10(b) than to that seen with the other analogues. Here, the luminescence intensity remained constant upon the addition of 0.3 equivalent of $\text{Tb}(\text{III})$, suggesting the formation of preliminary species resulting from the self-assembly of several ligands with $\text{Tb}(\text{III})$. Indeed, ligand **7** contains long and flexible pendant arms bearing four nitrogen atoms through its terminal moieties, which can easily form extra-cavities or allow the interpenetration of two ligands around the same metal centre. However, upon further addition of $\text{Tb}(\text{III})$, the displacement of the complexation equilibrium towards the stable formation of the host-guest system **7.Tb** was observed by the large increase in the terbium emission upon the addition of 0.9 equivalent of lanthanide ion. Finally, the formation of other minor species was detected via a quenching of the luminescence intensity within the addition of 1 → 5 equivalent of $\text{Tb}(\text{III})$. Despite the minor influence that the terminal moiety seemed to have on the photophysical properties of the complexes **L.Tb** ($\text{L} = \mathbf{3}, \mathbf{4}, \mathbf{5}, \mathbf{6}, \mathbf{7}$), the binding process was highly affected by the nature of the four pendant arms; hence, these spectroscopic titration studies have demonstrated the presence of the species **L.Tb** in solution and the potential formation of other different topologies at higher concentration of $\text{Tb}(\text{III})$.

Determination of the binding constants for the formation of **L.Tb** in solution

In order to highlight the complexation process, the data obtained from the titration above were further investigated using the non-linear regression analysis SPECFIT[®]. In each case, the luminescence data recorded above were fitted successfully, using various stoichiometries, with good convergence factors and the binding constants resulting from these fits are summarised in Table 2. It can be concluded from these results that in each case, the formation of the desired 1:1 stoichiometric species occurs. However, the speciation and the stability of the complexes formed seem to be influenced significantly by the nature of the pendant arms. For example, the fitting of the data obtained from the titrations of **3** and **4** with $\text{Tb}(\text{III})$ showed in both cases the major formation of the 1:1 stoichiometric species with $\text{Log } K_{11} = 8.2$ and 5.5 , respectively. The stable formation of the species **3₂.Tb** was also detected with $\text{Log } K_{12} = 5.2$; however, this indicates that the complex **3.Tb** is the most stable species present in solution.

The speciation distribution plot derived from these calculations, shown in Figure 11(a), indicated that the formation of the species **3₂.Tb** is maximal in the presence of 0.5 equivalents of $\text{Tb}(\text{III})$ in solution (66.4%) and that the equilibrium was displaced to the exclusive formation of **3.Tb** (89.5%) upon the addition of an equimolar ratio of lanthanide salt.

In the case of **4**, the convergence of the mathematical model could be reached only with the introduction of the 2:1 M/L species, for which the formation at high terbium

Table 2. Binding constant calculated from the fitting of the changes observed during the $\text{Tb}(\text{III})$ emission titrations of the calixarenes derivatives.

$\text{Log } \beta_{\text{ML}}$	3	4	6	7
$\text{Log } \beta_{1:1}$	8.2 ± 0.8	5.5 ± 0.2	7.8 ± 0.3	5.3 ± 0.1
$\text{Log } \beta_{2:1}$	–	6.8 ± 0.3	–	–
$\text{Log } \beta_{1:2}$	13.4 ± 0.9	–	13.5 ± 0.5	–
$\text{Log } \beta_{2:3}$	–	–	–	18.4 ± 0.1

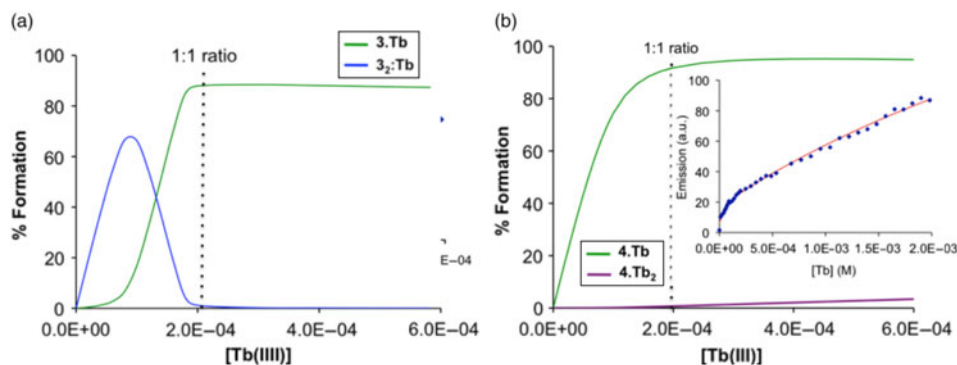


Figure 11. (Colour online) (a) Speciation distribution diagram describing the binding process of **3** with Tb(III). Inset: fits resulting from the fitting. (b) Speciation distribution diagram obtained for the complexation of Tb(III) with **4**. Inset: fits resulting from the fitting of the luminescence titration data.

concentration ($[Tb(III)] > 2 \times 10^{-4} M$) has been calculated to be very weak with $\text{Log } K_{21} = 1.4$. The speciation distribution plot describing the binding process of **4** with Tb(III) (as shown in Figure 11(b)) confirmed the expected behaviour, showing the unique formation of **4.Tb** in the presence of 1 equivalent of Tb(III), which is followed by the slow formation of the second less stable species **4.Tb₂**. The difference in behaviour between **3** and **4** can possibly be explained by the nature of the terminal amine moieties. The self-assembly of two ligands of **3** around the same terbium ion can potentially occur via tail-to-tail arrangement after rotation of one or several pendant arms. Nevertheless, the formation of the 1:2 M/L has not been observed in the case of **4**, which could be due to the configuration of the morpholinyl group, shielding the access to the metal centre and preventing the formation of multi-ligand species. Finally, the weak formation of the di-metallic species can also potentially occur through the complexation of a second terbium ion with the terminal oxygen atoms present on the morpholinyl group of **4**.

The influence of the nature of the pendant arms on the binding process was further confirmed by the fitting of the luminescence titration of ligands **6** and **7**, which despite

their structural similarities showed three different behaviours. In the case of ligand **6**, the results obtained were similar to those obtained for ligand **3**, which bears the same terminal moieties. The formation of two species **6₂.Tb** and **6.Tb** was detected. Moreover, the 1:2 stoichiometric complexes **6₂.Tb** were observed to be more favoured ($\text{Log } K_{12} = 5.60$) than in the case of the complexation of **3**, and reached a maximum formation of ca. 85.4% in the presence of 0.5 equivalents of terbium salt. This can be explained by the higher flexibility of the pendant arms, which can stabilise the self-assembly of ligands to fulfil the coordination requirement of the terbium ion. However, the formation of the **6.Tb** species was found to be predominant in solution upon the addition of an equimolar ratio of lanthanide ion ($> 95\%$ formation) as shown in Figure 12(a).

The calculations resulting from the luminescence emission titrations of **7** could also be fitted accurately by taking into account the formation of the secondary 2:3 M/L species, which does not correspond to the probable binding mode but more likely reflects the weak formation of minor secondary species, such as the formation of 1:2 or 3:2 M/L. Nevertheless, these results also showed the

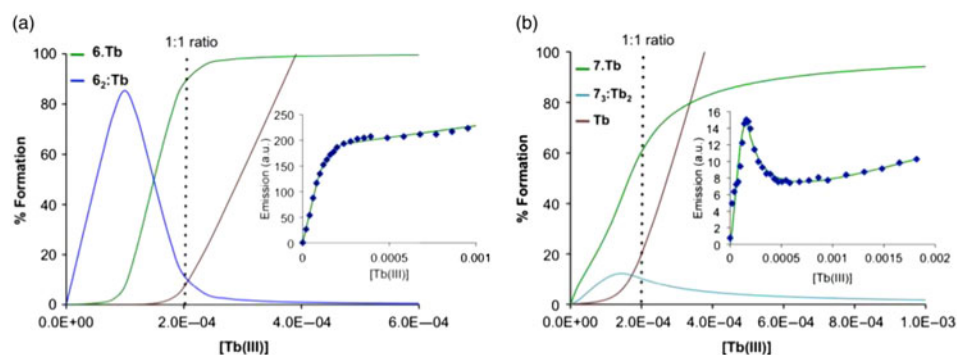


Figure 12. (Colour online) (a) Speciation distribution diagram describing the binding process of **6** with Tb(III). Inset: fits resulting from the fitting. (b) Speciation distribution diagram obtained for the complexation of Tb(III) with **7**. Inset: fits resulting from the fitting of the luminescence titration data.

predominant formation of the host–guest system **7.Tb** during the titration, with a binding constant of $\text{Log } K_{11} = 5.3$, which was in the same range as the one obtained for the formation of **4.Tb**.

It was clear from these results that the nature of the terminal moiety has a considerable influence on the binding process. Despite the difference of the length of their pendant arms, the calix[4]arenes derivatives **3** and **5**, which possess the same terminal piperidine terminal moieties, showed similar behaviour upon the addition of Tb(III). In both cases, the same two species **L₂.Tb** and **L.Tb** were formed with similar binding constant. Conversely, the Tb(III) titration of **4** and **7** showed that the nature of the terminal moiety can have a dramatic influence on the binding process. Even if in each case, the major formation of the 1:1 species has been observed, the binding constant associated with the formation of the **L.Tb** (**L** = **4**, **7**) complexes were found to be lower by three log units of magnitude than for **3.Tb** and the nature of the second species was also found to be influenced by the nature of the terminal moiety. Indeed, it was clear from these studies that the presence of donor atoms such as O and NH on position 6 of the cyclo-amine displaces the complexation equilibrium towards species containing several metal ions and was also seen to destabilise the complexes **L.Tb**.

Conclusion

In this work, we have proposed two novel alternative synthesis routes for the development of calix[4]arene derivatives tetra-alkylated on their lower rim with various amine groups; the synthesis of which was achieved in a simple manner. These structures were characterised using conventional methods and in some cases, using X-ray crystallography. We have shown that these tetra-amides form 1:1 complexes and that in solution that same species is the most dominated one, but other minor species can also be formed. All the complexes were shown to give rise to Tb(III)-centred emission upon excitation of the calixarene aryl units which function as antennae, where the shorter spaced and less flexible complexes (formed from ligands **3** and **4**) gave rise to significantly higher quantum yield of luminescence than those formed from the more flexible analogues. The changes from the Tb(III)-centred emission were then used to determine the binding affinity of these novel ligands for Tb(III) by fitting the changes in the Tb(III) emission using the non-linear regression analysis program. On all occasions, good fits were observed with moderate-to-high binding constants depending on the species formed. In summary, the result of this investigation shows that novel calix[4]arene aromatic core can be simply modified to allow for the formation of new lanthanide complexes possessing lanthanide ions, the

emission of which can be sensitised by excitation of the calix[4]arene aromatic core. We are in the process of modifying these structures further with the view of developing novel sensors and imaging agents based on modulation in lanthanide luminescence; particularly with the view of developing near infrared emitting complexes (**18**), and functional complexes for biological applications (**19**, **20**).

Supplemental data

Supplemental data for this article can be accessed here at <http://dx.doi.org/10.1080/10610278.2013.810339>.

References

- (1) (a) Bünzli, J.-C.G. *Chem. Rev.* **2010**, *110*, 2729–2755. (b) Thibon, A.; Pierre, V.C. *Anal. Bioanal. Chem.* **2009**, *394*, 107–120. (c) Montgomery, C.P.; Murray, B.S.; New, E.J.; Pal, R.; Parker, D. *Acc. Chem. Res.* **2009**, *42*, 925–937. (d) dos Santos, C.M.G.; Harte, A.J.; Quinn, S.J.; Gunnlaugsson, T. *Coord. Chem. Rev.* **2008**, *252*, 2512–2527. (e) Faulkner, S.; Pope, S.J.A.; Burton-Pye, B.P. *Appl. Spectrosc. Rev.* **2005**, *40*, 1–31. (f) Lincheneau, C.; Stomeo, F.; Comby, S.; Gunnlaugsson, T. *Aust. J. Chem.* **2011**, *64*, 1315–1326.
- (2) (a) Cantuel, M.; Lincheneau, C.; Buffeteau, T.; Jonusauskaite, L.; Gunnlaugsson, T.; Jonusauskas, G.; McClenaghan, N.D. *Chem. Commun.* **2010**, *46*, 2486–2488. (b) McMahon, B.K.; Mauer, P.; McCoy, C.P.; Lee, T.C.; Gunnlaugsson, T. *J. Am. Chem. Soc.* **2009**, *131*, 17542–17543. (c) Murray, N.S.; Jarvis, S.P.; Gunnlaugsson, T. *Chem. Commun.* **2009**, 4959–4961.
- (3) (a) Andrews, M.; Jones, J.E.; Harding, L.P.; Pope, S.J.A. *Chem. Commun.* **2011**, *47*, 206–207. (b) Shinoda S.; Tsukube H. *Analyst* **2011**, *136*, 431–435. (c) Chauvin, A.-S.; Comby, S.; Song, B.; Vandevyver, F.T.; Bünzli, J.-C. G. *Chem. Eur. J.* **2007**, *13*, 9515–9526.
- (4) (a) Kotova, O.; Comby, S.; Gunnlaugsson, T. *Chem. Commun.* **2011**, *47*, 6810–6812. (b) McMahon, B.K.; Gunnlaugsson, T. *Tetrahedron Lett.* **2010**, *51*, 5402–5405. (c) Nonat, A.M.; Harte, A.J.; Sénéchal-David, K.; Leonard, J.P.; Gunnlaugsson, T. *Dalton Trans.* **2009**, 4703–4711.
- (5) (a) Starynowicz, P.; Bukietynska, K.; Golab, S.; Ryba-Romanowski, W.; Sokolnicki, J. *Eur. J. Inorg. Chem.* **2002**, 2344–2347. (b) Bazin, H.; Triquet, E.; Mathis, G. *J. Biotechnol.* **2002**, *82*, 333–350. (c) Bünzli, J.C.G.; André, N.; Elhabiri, M.; Muller, G.; Piguët, C. *J. Alloys Comp.* **2000**, *303/304*, 66–74. (d) Alpha, B.; Lehn, J.-M.; Mathis, G. *Angew. Chem. Int. Ed. Eng.* **1987**, *26*, 266–267.
- (6) (a) Deiters, E.; Song, B.; Chauvin, A.S.; Vandevyver, C.D. B.; Gumy, F.; Bünzli, J.-C.G. *Chem. Eur. J.* **2009**, *15*, 885–900. (b) Koeller, S.; Bernardinelli, G.; Piguët, C. *C. R. Chim.* **2006**, *9*, 1158–1162. (c) Davies, G.M.; Adams, H.; Pope, S.J.A.; Faulkner, S.; Ward, M.D. *Photochem. Photobiol. Sci.* **2005**, *4*, 829–834. (d) Glover, P.B.; Ashton, P.R.; Childs, L.J.; Rodger, A.; Kercher, M.; Williams, R.M.; De Cola, L.; Pikramenou, Z. *J. Am. Chem. Soc.* **2003**, *125*, 9918–9919. (e) Fatin-Rouge, N.; Toth, E.; Perret, D.; Backer, R.H.; Merbach, A.E.; Bünzli, J.C.G. *J. Am. Chem. Soc.* **2000**, *122*, 10810–10820. (f) Renaud, F.; Piguët, C.;

- Bernardinelli, G.; Hopfgartner, G.; Bünzli, J.C.G. *Chem. Commun.* **1999**, 457–458.
- (7) (a) Butler, C.; Goetz, C.M.; Fitchett, P.E.; Krugger, P.E.; Gunnlaugsson, T. *Inorg. Chem.* **2011**, *50*, 2723–2725. (b) Li, X.X.; Wei, Z.Q.; Yue, S.T.; Wang, N.; Mo, H.H.; Liu, Y. L. *J. Chem. Cryst.* **2011**, *5*, 757–761. (c) Chen, W.T.; Fukuzumi, S. *Inorg. Chem.* **2009**, *48*, 3800–3807. (d) Wang, C.-G.; Xing, Y.-H.; Li, Z.-P.; Li, J.; Zeng, X.-Q.; Ge, M.-F.; Niu, S.-Y. *Cryst. Growth Des.* **2009**, *9*, 1525–1530. (e) Mazzanti, M.; Chen, X.Y.; Bretonniere, Y.; Pecaut, J.; Imbert, D.; Bünzli, J.C.G. *Inorg. Chem.* **2007**, *46*, 625–637. (f) Comby, S.; Scopelliti, R.; Imbert, D.; Charbonnière, L.J.; Ziessel, R.; Bünzli, J.C.G. *Inorg. Chem.* **2006**, *45*, 3158–3160. (g) Lincheneau, C.; Leonard, J.P.; McCabe, T.; Gunnlaugsson, T. *Chem. Commun.* **2011**, *47*, 7119–7121. (h) Leonard, J.P.; Jensen, P.; McCabe, T.; O'Brien, J.E.; Peacock, R.D.; Kruger, P.E.; Gunnlaugsson, T. *J. Am. Chem. Soc.* **2007**, *129*, 10986–10987.
- (8) (a) Matthews, S.E.; Parzuchowski, P.; Garcia-Carrera, A.; Gruttner, C.; Dozol, J.F.; Bohmer, V. *Chem. Commun.* **2001**, 417–418. (b) Barbosa, S.; Carrera, A.G.; Matthews, S.E.; Arnaud-Neu, F.; Bohmer, V.; Dozol, J.-F.; Rouquette, H.; Schwing-Weill, M.J. *J. Chem. Soc. Perkin Trans.* **1999**, *2*, 719–724.
- (9) (a) Aime, S.; Barge, A.; Botta, M.; Casnati, A.; Fragai, M.; Luchinat, C.; Ungaro, R. *Angew. Chem. Int. Ed.* **2001**, *40*, 4737–4739. (b) Schuhle, D.T.; Schatz, J.; Laurent, S.; Elst, L.V.; Muller, R.N.; Stuart, M.C.A.; Peters, J.A. *Chem. Eur. J.* **2009**, *15*, 3290–3296. (c) Georgiev, E.M.; Roundhill, D. M. *Inorg. Chim. Acta* **1997**, *258*, 93–96.
- (10) Sato, N.; Shinkai, S. *J. Chem. Soc. Perkin Trans.* **1993**, *2*, 621–624.
- (11) Sabbatini, N.; Guardigli, M.; Mecati, A.; Balzani, V.; Ungaro, R.; Ghidini, E.; Casnati, A.; Pochini, A. *J. Chem. Soc. Chem. Commun.* **1990**, 878–879.
- (12) Ohto, K.; Yano, M.; Inoue, K.; Nagasaki, T.; Goto, M.; Nakashio, F.; Shinkai, S. *Polyhedron* **1997**, *16*, 1655–1661.
- (13) Georgiev, E.M.; Clymire, J.; McPherson, G.L.; Roundhill, D.M. *Inorg. Chim. Acta* **1994**, *227*, 293–296.
- (14) Pappalardo, S.; Bottino, F.; Giunta, L.; Pietraszkiewicz, M.; Kappiuk, J. *J. Incl. Phenom. Mol. Recogn.* **1991**, *10*, 387–392.
- (15) Ulrich, G.; Ziessel, R.; Manet, I.; Guardigli, M.; Sabbatini, N.; Fraternali, F.; Wipff, G. *Chem. Eur. J.* **1997**, *3*, 1815–1822.
- (16) Froidevaux, P.; Harrowfield, J.M.; Sobolev, A.N. *Inorg. Chem.* **2000**, *39*, 4678–4687.
- (17) (a) Steemers, F.J.; Verboom, W.; Reinhoudt, D.N.; van der Tol, E.B.; Verhoeven, J.W. *J. Am. Chem. Soc.* **1995**, *117*, 9408–9414. (b) Zhang, N.; Tang, S.-H.; Liu, Y. *Spectrochim. Acta A* **2003**, *57*, 1107–1112.
- (18) (a) D'Alessio, D.; Muzzioli, S.; Skelton, B.W.; Stagni, S.; Massi, M.; Ogden, M.I. *Dalton Trans.* **2012**, *41*, 4736–4739. (b) Ennis, B.W.; Muzzioli, S.; Reid, B.L.; D'Alessio, D.M.; Stagni, S.; Brown, D.H.; Ogden, M.I.; Massi, M. *Dalton Trans.* **2013**, *42*, 6894–6901. (c) Driscoll, C.R.; Reid, B.L.; McIlldowie, M.K.; Muzzioli, S.; Nealon, G.L.; Skelton, B.W.; Stagni, S.; Brown, D.H.; Massi, M.; Ogden, M.I. *Chem. Commun.* **2011**, *47*, 3876–3878.
- (19) Oueslati, I.; SaFerreira, R.A.; Carlos, L.D.; Baleizao, C.; Berberan-Santos, M.N.; de Castro, B.; Vicens, J.; Pischel, U. *Inorg. Chem.* **2006**, *45*, 2652–2660.
- (20) Gutsche, C.D.; Lin, L.G. *Tetrahedron* **1986**, *42*, 1633–1640.
- (21) (a) Comby, S.; Tuck, S.A.; Truman, L.K.; Kotova, O.; Gunnlaugsson, T. *Inorg. Chem.* **2012**, *51*, 10158–10168. (b) Molloy, J.K.; Kotova, O.; Peacock, R.D.; Gunnlaugsson, T. *Org. Biomol. Chem.* **2012**, *10*, 314–322.
- (22) Iwamoto, K.; Shinkai, S. *J. Org. Chem.* **1992**, *57*, 7066–7073.